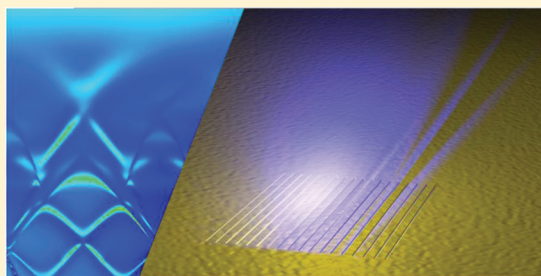# Low-Temperature Plasmonics of Metallic Nanostructures

Jean-Sebastien G. Bouillard,* Wayne Dickson, Daniel P. O'Connor, Gregory A. Wurtz, and Anatoly V. Zayats

Nano-optics and Near-field Spectroscopy Laboratory, Department of Physics, King's College London, Strand, London WC2R 2LS, United Kingdom

S *Supporting Information*

ABSTRACT: The requirements for spatial and temporal manipulation of electromagnetic fields on the nanoscale have recently resulted in an ever-increasing use of plasmonics for achieving various functionalities with superior performance to those available from conventional photonics. For these applications, ohmic losses resulting from free-electron scattering in the metal is one major limitation for the performance of plasmonic structures. In the low-frequency regime, ohmic losses can be reduced at low temperatures. In this work, we study the effect of temperature on the optical response of different plasmonic nanostructures and show that the extinction of a plasmonic nanorod metamaterial can be efficiently controlled with temperature with transmission changes by nearly a factor of 10 between room and liquid nitrogen temperatures, while temperature effects in plasmonic crystals are relatively weak (transmission changes only up to 20%). Because of the different nature of the plasmonic interactions in these types of plasmonic nanostructures, drastically differing responses (increased or decreased extinction) to temperature change were observed despite identical variations of the metal's permittivity.

KEYWORDS: *Surface plasmons, low-temperature effects, plasmonic metamaterials, plasmonic crystals*

P lasmonic excitations on smooth and nanostructured surfaces are very sensitive to variations of the permittivity of the metal as well as the adjacent dielectric.[1-4] The impact of both the real and imaginary parts of the metal and the embedding dielectric's permittivity are important and have been used in the past to achieve all-optical, electro-optical, thermo-optical, and magneto-optical control of the plasmonic excitations and respective tunability of their spectral response.[5-10] While the majority of these effects rely on the modification of the permittivity of the adjacent dielectric, changing the permittivity of the metal is also important for all-optical effects based on metal nonlinearities,[11-13] sensing applications and the possibility to reduce ohmic losses, if the control of electron scattering can be achieved. Numerous attempts to engineer plasmonic materials with improved losses compared to Au or Ag have been made by using various alloys or unconventional plasmonic materials to control the complex permittivity of the structure, since both components influence the resonant behavior and loss in plasmonic nanostructures.[14-16] A hitherto unexplored way to manage these parameters is temperature control.

Static and low-frequency conductivity of metals increases at low temperatures due to the decrease in electron−phonon and electron−electron scattering. In the optical frequency range, temperature effects influence the metal's permittivity via the modification of both the inter- and intraband electron scattering.[17] The temperature effects due to nonequilibrium temperature distributions of electrons and phonons are also often used to describe both energy relaxation pathways and the

ultrafast optical properties of metals in transient optical measurements. Moreover, depending on the application, ohmic losses influence not only the energy dissipation for guided plasmonic excitations but also the quality factor of the plasmonic resonances in nanoparticles and crystals, imaging quality when using using plasmonic super- and hyperlenses which are strongly dependent on the interaction between the plasmonic components of metamaterials, allowing or preventing the manifestation of nonlocal effects.

Here we investigate the effect of temperature on the optical properties of two different types of plasmonic nanostructures: a gold-nanorod metamaterial and plasmonic crystals made in gold thin-films. These structures exhibit distinctively different temperature-dependent optical properties: an increased transmission for metamaterials due to a decreased extinction cross-section, and a decreased transmission for plasmonic crystal due to losses in the metal. Numerical modelling was used to describe the temperature-dependent permittivity of the metal, taking into account the temperature-dependence of both the plasma frequency and the electron damping rates. The experimental observations were fully recovered using this model without any fitting parameters. The simulated temperature-dependent values have then been used to predict the low-temperature performance of various plasmonic components.

The plasmonic nanorod metamaterial studied in the first part of this work (Figure 1) is produced electrochemically as
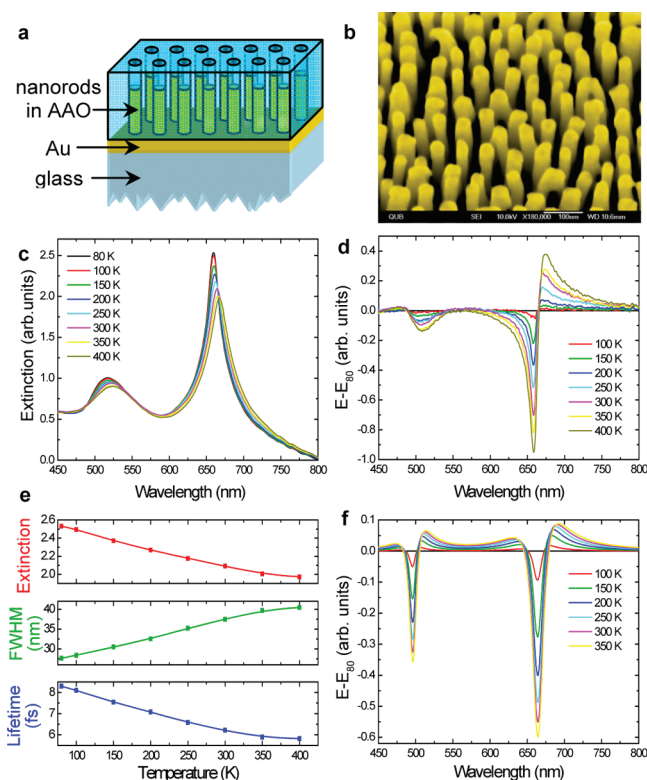

Figure 1. Temperature-dependent optical properties of plasmonic nanorod metamaterial. (a) Schematics and (b) SEM image of the sample. Experimental extinction spectra (c) measured at different temperatures and differential extinction with respect to 80 K temperature (d). (e) Temperature dependence of the extinction, line-width and relaxation time recovered from the experiment. (f) Simulated temperature dependence of the differential extinction spectra.

described in the Supporting Information. The resulting structure that consists of an array of aligned Au nanorods is an example of a plasmonic metamaterial with optical properties tunable throughout the visible and near-infrared spectral range that exhibits a variety of interesting properties such as hyperbolic dispersion, negative refraction, and room-temperature nonlocal effects.[18−22] These properties are crucial for the implementation of novel waveguiding, sensing, and imaging architectures. In the visible spectral range, the metamaterial's properties are determined by the strong interaction between the closely spaced (~50 nm) Au nanorods (25 nm diameter, 300 nm length) that results in the formation of collective plasmonic modes associated with electron movement either along (L-mode) or perpendicular to (T-mode) the nanorod long axis.[22,23] These modes are observed as strong extinction peaks in the transmission spectra of the arrays (Figure 1c).

Both the transverse and longitudinal resonances decrease in amplitude and broaden in width as the temperature increases. The change in extinction is also accompanied by a spectral shift of both resonances toward longer wavelengths (Figure 1c). Due to the metal's dispersion, temperature effects are more pronounced for the longitudinal than the transverse resonance. A change in the line width greater than 40% with the associated extinction change of approximately 30% (transmission

decreases by almost a factor of 10 when the temperature is decreased from 400 to 80 K) is observed for the longitudinal resonance, compared to a 10% change in both quantities for the transverse mode resonance. Note that these resonances are not sensitive to the superstrate for the nanorods embedded in the matrix[20,23] and thus are not affected by possible temperature-dependent adsorption of residual vapors in the vacuum chamber.

Taking into account the temperature-dependent Au permittivity, described within the Drude approximation, all the features of the observed behavior of the plasmonic metamaterials can be modeled (Figure 1f). Please note that the temperature-dependent permittivity model used is valid for wavelengths above 550 nm away from the interband electron transition in Au, see Supporting Information for details; thus, only the temperature dependence of the L-mode will be discussed here. While the relative variation $\Delta \text{Re}(\varepsilon_m)/\text{Re}(\varepsilon_m)$ variation of the real part of the metal's permittivity of Au is small (~0.02) and has a comparatively weak effect on the extinction, a substantial increase of $\text{Im}(\varepsilon_m)$ by approximately a factor of 2 at 750 nm is estimated between 80 and 350 K (as shown in Supporting Information). The change in the electron distribution near the Fermi level and the associated increased electron scattering rate as the electron and phonon temperature increases leads to an increase in the imaginary part of Au permittivity, resulting in a lowered quality factor of the plasmonic resonances. This in turn leads to the increased transmission as radiative losses are increased. The decreased lifetime of the dipolar resonances translates into a decreased inter-rod coupling determining the L-mode wavelength, redshifting its spectral position by about 8 nm for an angle of incidence of 45°, a value that was found to be highly dependent on the metamaterial geometry. On the basis of the model calculations, the change in the electron−phonon scattering rate from ~0.5×10^{14} s^{-1} at 80 K to ~2×10^{14} s^{-1} at 350 K is the dominating contribution to the observed change in the metamaterial extinction with electron−electron scattering processes staying at an almost constant level of ~1×10^{14} s^{-1} over the same temperature range at a wavelength of 650 nm. This temperature behavior of electron scattering is expected at the thermal equilibrium when the temperature changes are slow.

The observed temperature dependence of the optical properties of periodically structured metal films (plasmonic crystals) shows a different behavior from that of the nanorod metamaterial. With the temperature-induced increase of the ohmic losses, the overall transmission of plasmonic crystals becomes smaller. This is due to a different mechanism of plasmonic coupling, mediated by surface plasmon polaritons rather than localized surface plasmons as in the case of the nanorod metamaterial.

The plasmonic crystal under investigation consists of a periodic set of slits (width 75 nm, period 550 nm) perforated in a 200 nm thick Au film deposited on a glass substrate (Figure 2, see Supporting Information for details of the fabrication process). The crystal was covered by a protective bilayer consisting of a 100 nm layer of Ta_2O_5 and a 2000 nm layer of PMMA. This prevents variations in the optical properties of the crystal associated with the temperature-dependent adsorption of residual vapors present in the vacuum chamber of the cryostat. Without this protective layer, vapor adsorption forms a nanoscopic layer on the crystals resulting in modifications to the crystal's eigenmodes due to changes in the refractive index
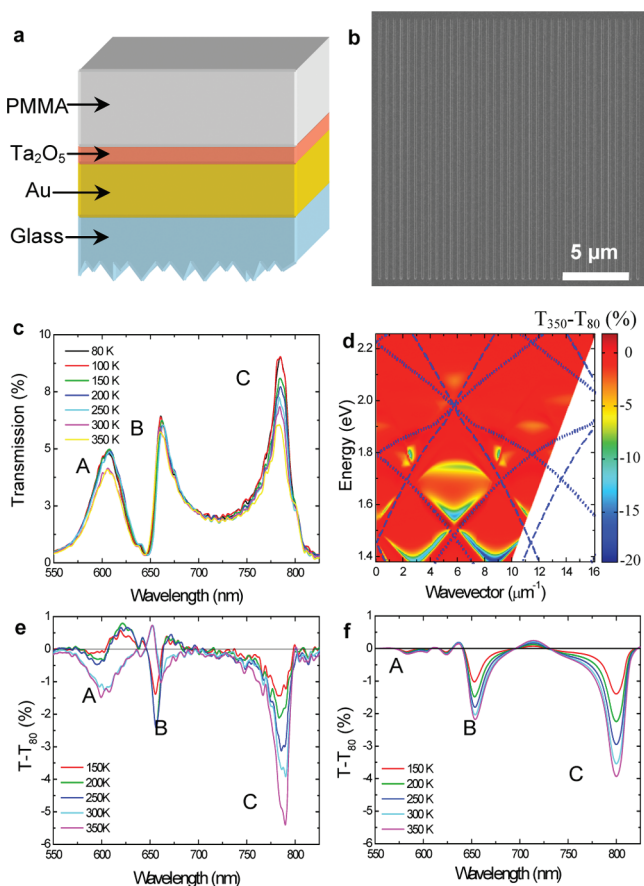
Figure 2. Temperature-dependent optical properties of plasmonic crystals. (a) Schematics and (b) SEM image of the sample. (c) Experimental transmission spectra of the SPP crystal at different temperatures. (d) Simulated differential dispersion of the crystal transmission ($T_{350}-T_{80}$) along with the calculated position of the Bragg diffracted SPP modes obtained in the smooth film approximation for refractive indices of the adjacent dielectric of 1.5 (blue dashed line) and 2.1 (blue dotted line)). (e,f) Differential transmission with respect to the transmission at 80 K temperature: (e) experiment and (f) simulations.

of the superstrate medium. The resulting modification in the crystal's optical properties is illustrated in the Supporting Information (Figure S2). This effect is the basic principle upon which biosensors are designed with plasmonic crystals[24] and can be used after appropriate calibration as a highly sensitive sensor of vapor absorption/desorption.

The transmission spectra of the SPP crystal under investigation are shown in Figure 2 for various temperatures. The transmission spectra are mainly determined by the SPP−Bloch modes supported by the periodic structure with minima due to the band-gap formation (see Figure 2d for a complete dispersion of the crystal). At the Brillouin zone boundaries, counter-propagating SPP−Bloch modes interfere destructively to produce local band-gaps.[3,7] From Figure 2c,d, one can observe that the main effect of temperature increase is a net decrease in the crystal's transmission. This comes in sharp contrast with the previously discussed behavior of the metamaterial for which the transmission increases with temperature for the L-mode. A more subtle response of the crystal to the temperature increase is reflected in the spectral position of the maxima observed in transmission that display either red- or blue-wavelength shifts, depending on the mode

considered, while SPP band-gaps consistently experience a red shift. The temperature effects in plasmonic crystals are much smaller with only a few percent change in the transmission at normal incidence and about 20% at oblique incidence where the strongest effect is observed.

These observations are consistent with the results obtained in the simulations based on the experimental crystal's geometry and using the same temperature-dependent model for the permittivity of Au which was used for the metamaterial. The simulations reproduce all the main experimental observations (Figure 2e,f). Again, the model shows that as the temperature of the crystal increases so do both the real $\mathrm{Re}(\varepsilon)$ and the imaginary $\mathrm{Im}(\varepsilon)$ parts of the metal's permittivity. Both of these quantities affect the transmittance of the crystal. In particular, numerical calculations demonstrate that the decrease of the crystal's transmission is mainly due to the reduction of the coupling of SPP modes across the film interfaces. This mechanism, which depends on the SPP−Bloch mode lifetime, is affected by the increase in $\mathrm{Im}(\varepsilon)$ with temperature. The small shift of the band gap toward longer wavelengths reflects the increase in $\mathrm{Re}(\varepsilon)$ with temperature although the increased losses in the metal compensate partially the influence of the $\mathrm{Re}(\varepsilon)$ variations on the band gap position. In Figure 2c, two band-gaps are visible corresponding to the $(\pm 2,0)$ mode at the superstrate interface and the $(\pm 1,0)$ mode at the substrate interface at the free-space wavelengths of approximately 650 and 850 nm, respectively. As can be observed in Figure 2c, no detectable change in the position of the $(\pm 1,0)_{sub}$ band gap can be seen, while the $(\pm 2,0)_{super}$ band gap exhibits a small but distinguishable 5 nm red shift with temperature increase. This is in agreement with the results from the model calculations, which show that over the temperature range considered the relative change in the real part of the smooth film SPP wavenumber, which approximately determines the center-wavelength of the band gap at a free-space wavelength corresponding to the $(\pm 2,0)_{super}$ band gap location of 650 nm, is about an order of magnitude smaller than that corresponding to the location of the $(\pm 1,0)_{sub}$ band gap at around 850 nm due to the difference in the relative changes of $\mathrm{Im}(\varepsilon)$.

It should be noted that under the conditions of the present study, thermal expansion effects of materials are small in both the metamaterial and SPP crystal (see Supporting Information for details) but may influence the band gap position in the crystal since these are extremely sensitive to the geometry of the structure.[6−8,24] In any case, the effects of temperature on the optical properties of plasmonic crystals are less pronounced than for plasmonic nanorod metamaterials, but they are more sensitive to the temperature dependence of $\mathrm{Re}(\varepsilon)$.

The measured temperature-dependent optical properties determined by monitoring plasmonic excitations in various types of nanostructures show that different plasmonic nanostructures exhibit different responses to temperature changes despite relying on the same modification of the metal permittivity with temperature. This is due to the different nature of plasmonic interactions in the nanostructures considered. The observed temperature behavior has been modeled within the Drude approximation for the metal permittivity without any fitting parameters and allows the prediction of temperature effects in various plasmonic devices such as waveguides, sensors, superlenses, and transformation optics where low working temperature can lead to the performance improvement of the devices.

The temperature-dependent model of the permittivity of Au validated in the presented examples allows for the evaluation of a temperature dependence of various plasmonic devices properties. First, we consider the temperature dependence of the SPP propagation length (L_{SPP}) on smooth metal films and waveguides. The observed change in $\text{Im}(\varepsilon)$ is about 3-fold, which is almost independent of the spectral position within the 80−400 K temperature range considered. A relatively small increase in $\text{Re}(\varepsilon)$ of about 2% does not significantly influence either the SPP's spectral position or its field confinement. Therefore, L_{SPP} on a smooth interface is mainly determined by $L_{SPP} \sim 1/\text{Im}(\varepsilon)$ and the SPP propagation length increases by about 200% by moving from room temperature to 80 K (Figure 3). Similarly, for localized surface plasmons, $\text{Im}(\varepsilon)$ determines
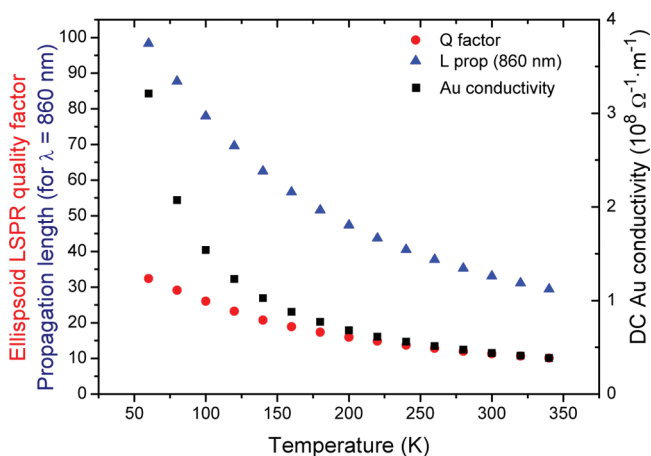

Figure 3. Temperature dependences of some chosen plasmonic devices characteristics. Simulated dependences of SPP propagation length at 860 nm wavelength, Q-factor of a Au ellipsoids at a wavelength of 860 nm, and the experimental DC conductivity of bulk Au.[25]

the quality factor of the resonance $Q_{LSP} \sim 1/\text{Im}(\varepsilon)$ which can be improved by about 3 times at low temperatures. The same argument is also valid for quality factors determining the sensitivity of both LSPR and SPR sensors as well as devices based on transformation optics, while a low-temperature improvement in superlensing, where ohmic losses limit image resolution, may be somewhat smaller owing to the $\ln(\text{Im}(\varepsilon))$ dependence.[14] Nevertheless, the observed drastically different temperature behaviors of the plasmonic systems show that to estimate the temperature dependent performance of the plasmonic nanostructures, one should consider not only the permittivity dependence but also the plasmonic interaction within the nanostructure should be considered. Experiments with plasmonic structures incorporating semiconducting materials, such as nanolasers, amplifiers, and mid-IR emitting devices may benefit from low temperatures due to both the optical properties of semiconductors and plasmonic properties improvement at low temperatures with the resulting effect depending on the type of nansotructure considered.[26,27]

In addition to these applications, the findings are important for the understanding of electron scattering in plasmonic materials and the interpretation of time-resolved measurements. The knowledge of temperature dependent permittivity may also provide insights into nonlinear and ultrafast optical properties of metals as hot electrons play a major role in them. It should however be noted that the difference between

nonlinear and temperature-dependent properties studied here is the nonequilibrium state between the lattice and the electron gas under ultrafast excitation and equilibrium (the lattice and the electron gas have the same temperature) state in the temperature-dependent measurements presented here.

■ ASSOCIATED CONTENT

Ⓢ Supporting Information

Sample fabrication (Au nanorod metameterial, Au plasmonic crystals), low-temperature optical measurements, finite element modeling of optical properties of plasmonic metamaterials and plasmonic crystals, model of the temperature dependent permittivity of Au, thermal expansion effects, and vapor adsorption effects on the optical properties of plasmonic crystals. This material is available free of charge via the Internet at http://pubs.acs.org.

■ AUTHOR INFORMATION

Corresponding Author

*E-mail: jean-sebastien.bouillard@kcl.ac.uk.

Notes

The authors declare no competing financial interest.

■ ACKNOWLEDGMENTS

■ REFERENCES

(1) Barnes, W. L.; Dereux, A.; Ebbesen, T. W. Surface plasmon subwavelength optics. *Nature* **2003**, *424*, 824−830.

(2) Lal, S.; Link, S.; Halas, N. J. Nano-optics from sensing to waveguiding. *Nat. Photonics* **2007**, *1*, 641−648.

(3) Zayats, A. V.; Smolyaninov, I. I.; Maradudin, A. A. Nano-optics of surface plasmon polariton. *Phys. Rep.* **2005**, *408*, 131−314.

(4) Lukyanchuk, B.; Zheludev, N. I.; Maier, S. A.; Halas, N. J.; Nordlander, P.; Giessen, H.; Chong, C. T. The Fano resonance in plasmonic nanostructures and metamaterials. *Nat. Mater.* **2010**, *9*, 707−715.

(5) Krasavin, A. V.; MacDonald, K. F.; Zheludev, N. I. High-contrast modulation of light with light by control of surface plasmon polariton wave coupling. *Appl. Phys. Lett.* **2004**, *85*, 3369−3371.

(6) Wurtz, G. A.; Pollard, R.; Zayats, A. V. Optical bistability in nonlinear surface-plasmon polaritonic crystals. *Phys. Rev. Lett.* **2006**, *97*, 057402−1−057402−4.

(7) Dickson, W.; Wurtz, G. A.; Evans, P. R.; Pollard, R. J.; Zayats, A. V. Electronically Controlled Surface Plasmon Dispersion and Optical Transmission through Metallic Hole Arrays Using Liquid Crystal. *Nano Lett.* **2008**, *8*, 281−286.

(8) Wurtz, G. A.; Hendren, W.; Pollard, R.; Atkinson, R.; Le Guyader, L.; Kirilyuk, A.; Rasing, T.; Smolyaninov, I. I.; Zayats, A. V Controlling optical transmission through magneto-plasmonic crystals with an external magnetic field. *New J. Phys.* **2008**, *10*, 105012.

(9) Nikolajsen, T.; Leosson, K.; Bozhevolnyi, S. I. Surface plasmon polariton based modulators and switches operating at telecom wavelengths. *Appl. Phys. Lett.* **2004**, *85*, 5833.

(10) Clavero, C.; Yang, K.; Skuza, J. R.; Lukaszew., R. A. Magnetic-field modulation of surface plasmon polaritons on gratings. *Opt. Lett.* **2010**, *35*, 1557−1559.

(11) Rotenberg, N.; Betz, M.; van Driel, H. M. Ultrafast control of grating-assisted light coupling to surface plasmons. *Opt. Lett.* **2008**, *33*, 2137−2139.

(12) MacDonald, K. F.; Sámson, Z. L.; Stockman, M. I.; Zheludev, N. I. Ultrafast active plasmonics. *Nat. Photonics* **2009**, *3*, 55−58.

(13) Wurtz, G. A.; Pollard, R.; Hendren, W.; Wiederrecht, G. P.; Gosztola, D. J.; Podolskiy, V. A.; Zayats, A. V. Designed ultrafast optical nonlinearity in a plasmonic nanorod metamaterial enhanced by nonlocality. *Nat. Nanotechnol.* **2011**, *6*, 107.

(14) West, P. R.; Ishii, S.; Naik, G. V.; Emani, N. K.; Shalaev, V. M.; Boltasseva, A. Searching for better plasmonic materials. *Laser Photonics Rev.* **2010**, *4*, 795.

(15) Khurgin, J. B.; Sun, G. In search of the elusive lossless metal. *Appl. Phys. Lett.* **2010**, *96*, 181102.

(16) Pelton, M.; Aizpurua, J.; Bryant, G. Metal-nanoparticle plasmonics. *Laser Photon Rev.* **2008**, *2*, 136.

(17) Liu, M.; Pelton, M.; Guyot-Sionnest, P. Reduced damping of surface plasmons at low temperatures. *Phys. Rev. B* **2009**, *79*, 035418.

(18) Pollard, R. J.; Murphy, A.; Hendren, W. R.; Evans, P. R.; Atkinson, R.; Wurtz, G. A.; Zayats, A. V. Optical nonlocalities and additional waves in epsilon-near-zero metamaterials. *Phys. Rev. Lett.* **2009**, *102*, 127405.

(19) Yao, J.; Liu, Z.; Liu, Y.; Wang, Y.; Sun, C.; Bartal, G.; Stacy, A. M.; Zhang, X. Optical Negative Refraction in Bulk Metamaterials of Nanowires. *Science* **2008**, *321*, 930.

(20) Kabashin, A. V.; Evans, P.; Pastkovsky, S.; Hendren, W.; Wurtz, G. A.; Atkinson, R.; Pollard, R.; Podolskiy, V. A.; Zayats, A. V. Plasmonic nanorod metamaterials for biosensing. *Nat. Mater.* **2009**, *8*, 867−871.

(21) Elser, J.; Wangberg, R.; Podolskiy, V. A.; Narimanov, E. Nanowire metamaterials with extreme optical anisotropy. *Appl. Phys. Lett.* **2006**, *89*, 261102.

(22) Wurtz, G. A.; Dickson, W.; O'Connor, D.; Atkinson, R.; Hendren, W.; Evans, P.; Pollard, R.; Zayats, A. V. Guided plasmonic modes in nanorod assemblies: strong electromagnetic coupling regime. *Opt. Express* **2008**, *16*, 7460−7470.

(23) Dickson, W.; Wurtz, G. A.; Evans, P.; O'Connor, D.; Atkinson, R.; Pollard, R.; Zayats, A. V. Dielectric-loaded plasmonic nano-antenna arrays: a metamaterial with tuneable optical properties. *Phys. Rev. B* **2007**, *76*, 115411.

(24) Stewart, M. E.; Mack, N. H.; Malyarchuk, V.; Soares, J. A. N. T.; Lee, T. −W.; Gray, S. K.; Nuzzo, R. G.; Rogers, J. A. Quantitative multispectral biosensing and 1D imaging using quasi-3D plasmonic crystals. *Proc. Natl. Acad. Sci. U.S.A.* **2006**, *103*, 17143−17148.

(25) Lide, D. R. Handbook of Chemistry and Physics, 75th ed; CRC Press: New York, 1996−1997; pp 11−14.

(26) Oulton, R. F.; Sorger, V. J.; Zentgraf, T.; Ma, R. −M.; Gladden, C.; Dai, L.; Bartal, G.; Zhang, X. Plasmon lasers at deep subwavelength scale. *Nature* **2009**, *461*, 629−632.

(27) Hill, M. T.; Oei, Y. −S.; Smalbrugge, B.; Zhu, Y.; De Vries, T.; Van Veldhoven, P. J.; Van Otten, F. W. M.; Eijkemans, T. J.; Turkiewicz, J. P.; De Waardt, H.; Geluk, E. J.; Kwon, S.-H.; Lee, Y.-H.; Nötzel, R.; Smit, M. K. Lasing in metallic-coated nanocavities. *Nat. Photonics* **2007**, *1*, 589−594.